miR-519d-3p released by human blastocysts negatively regulates endometrial epithelial cell adhesion by targeting HIF1α

XIAODAN WANG[1,2], SUIBING MIAO[2], LINQI LU[2], JINGCHUAN YUAN[2], SHUHONG PAN[2] and XIAOHUA WU[1,2]

[1]Department of Obstetrics and Gynecology, Hebei Medical University; [2]Reproductive Medicine Center, The Fourth Hospital of Shijiazhuang Affiliated to Hebei Medical University, Shijiazhuang, Hebei 050000, P.R. China

Received January 30, 2022; Accepted July 4, 2022

DOI: 10.3892/ijmm.2022.5179

Abstract. Successful embryo implantation requires a competent embryo, a receptive endometrium and synchronized communication between them. The selection of embryos with the highest implantation potential remains a challenge in the field of assisted reproductive technology. Moreover, little is known about the precise molecular mechanisms underlying embryo-endometrium crosstalk. MicroRNAs (miRNAs/miRs) have been detected in the spent embryo culture medium (SCM); however, their functions at the preimplantation stage remain unclear. In the present study, human SCM samples were collected during *in vitro* fertilization/intracytoplasmic sperm injection-embryo transfer and divided into implanted and not-implanted groups according to the clinical pregnancy outcomes. Total RNA was extracted and six miRNAs (miR-372-3p, miR-373-3p, miR-516b-5p, miR-517a-3p, miR-519d-3p and miR-520a-3p) were selected for reverse transcription-quantitative PCR (RT-qPCR) analysis. The results revealed that miR-372-3p and miR-519d-3p were markedly increased in SCM from blastocysts that failed to implant compared with in blastocysts that implanted. The receiver operating characteristic curve analysis revealed that miR-519d-3p was superior to miR-372-3p in predicting pregnancy outcomes. *In vitro* miRNA uptake and cell adhesion assays were performed to determine whether miR-519d-3p could be taken up by endometrial epithelial cells and to examine the biological roles of miR-519d-3p after internalization. Potential targets of miR-519d-3p were verified using a dual-luciferase reporter system. The results demonstrated that miR-519d-3p was taken up by human endometrial epithelial cells and that it may inhibit embryo adhesion by targeting HIF1α. Using RT-qPCR, western blot analysis and flow cytometry assay, HIF1α was shown to inhibit the biosynthesis of fucosyltransferase 7 and sialyl-Lewis X (sLe^x), a cell-surface oligosaccharide that serves an important role in embryonic apposition and adhesion. In addition, a mouse model was established and the results suggested that miR-519d-3p overexpression hampered embryo implantation *in vivo*. Taken together, miRNAs in SCM may serve as novel biomarkers for embryo quality. Furthermore, miR-519d-3p was shown to mediate embryo-endometrium crosstalk and to negatively regulate embryo implantation by targeting HIF1α/FUT7/sLe^x pathway.

Correspondence to: Dr Xiaohua Wu, Reproductive Medicine Center, The Fourth Hospital of Shijiazhuang Affiliated to Hebei Medical University, 206 East Zhongshan Road, Shijiazhuang, Hebei 050000, P.R. China
E-mail: xiaohuawu65@126.com

Key words: microRNAs, HIF1α, spent embryo culture medium, fucosyltransferase 7, sialyl-Lewis X, embryo implantation, endometrial epithelial cells

Introduction

Infertility has become a major medical and social problem affecting 12-15% of reproductive-age couples worldwide (1). Embryo implantation failure is considered the leading cause of infertility following natural conception and assisted reproductive technology (ART). Despite the major advances in reproductive medicine over the last few decades, especially *in vitro* fertilization (IVF)/intracytoplasmic sperm injection (ICSI)-embryo transfer (ET), implantation failure is still a rate-limiting process for a successful pregnancy (2). Embryo implantation is a complex event involving the apposition and adhesion of a competent embryo to the endometrial epithelium, followed by invasion into the underlying stroma (3). Selecting high-quality embryos for transfer and elucidating the molecular mechanisms underlying embryo implantation may aid in improving pregnancy outcomes.

Embryos enter the uterine cavity at embryonic day (D)4, approximately 48 or 72 h before implanting (4). During this time, the preimplantation embryos interact with the endometrium through soluble factors, including cytokines and growth factors, in preparation for implantation (5). For example, embryos that reach the blastocyst stage can induce upregulation of integrin β3 in human endometrial epithelial cells through the embryonic IL-1 system (6). Similarly, endometrium-secreted molecules internalized by the trophectoderm can lead to the expression of genes involved in embryo adhesion (7). However, due to the complexity of human embryo implantation, as well as ethical concerns, the intricate physiological and molecular processes remain unclear.

MicroRNAs (miRNAs/miRs) are a class of small non-coding RNA molecules, which have attracted extensive

attention for two specific reasons. Firstly, extracellular miRNAs that are extensively present in body fluids are highly resistant to biological and mechanical damage, and have been proposed as potential non-invasive biomarkers for various diseases (8-10). Secondly, miRNAs exported from donor cells can be internalized by recipient cells, where they modify gene expression and mediate intercellular communication (11). Emerging evidence has strongly suggested that miRNAs released by embryos may participate in various signaling pathways related to embryo implantation (12,13). Cuman *et al* (14) provided direct evidence for miRNA-mediated embryo-endometrium interactions. In this previous study, miR-661 was highly expressed in spent embryo culture medium (SCM) (i.e. the used embryo culture medium, which is discarded as waste following embryo culture) from human blastocysts that failed to implant, and inhibited embryo adhesion by targeting PVRL1 after being internalized by endometrial epithelial cells. However, research on embryo-released miRNAs is limited, and their physiological roles remain largely unknown.

In a previous microarray analysis, miR-516b-5p, miR-517a-3p, miR-519d-3p and miR-520a-3p were detected in SCM (15,16). Belonging to the chromosome 19 miRNA cluster (C19MC), these miRNAs have been reported to be exclusively expressed in the placenta and undifferentiated cells, and to participate in embryonic development and the progression of pregnancy (17). As exosome-carried miRNAs, they can mediate placental-maternal signaling after being released from trophoblasts. For example, placental trophoblasts have been shown to confer viral resistance to nonplacental recipient cells via the delivery of miR-516b-5p and miR-517a-3p (18). In addition, the involvement of miR-516b-5p and miR-520a-3p has been suggested in lipid and glucose homeostasis, and nervous system development of the fetus (19). Placenta-derived miR-517a-3p (20) and miR-519d-3p (21) may also contribute to the fetal-maternal immune tolerance. In the present study, miR-372-3p and miR-373-3p from the miR-371-373 cluster (which have been suggested to share a common ancestor and to work synergistically with the C19MC during pregnancy) were also assessed (22). According to the aforementioned findings, the present study hypothesized that these miRNAs in SCM may mediate embryo-endometrium crosstalk at the preimplantation stage and serve a role in embryo implantation.

Materials and methods

SCM sample collection. A total of 112 patients who underwent routine IVF/ICSI-ET at The Fourth Hospital of Shijiazhuang Affiliated to Hebei Medical University (Hebei, China) were recruited between March and December 2020; from these patients, 162 embryos that developed to the blastocyst stage were included. Briefly, all embryos were individually cultured in sequential media (Vitrolife AB) by specialized technicians in accordance with clinical procedures. On D3 after fertilization, embryos were transferred from G-1™ PLUS to G-2™ PLUS medium and cultured until blastocyst formation. On D5, blastocysts were assessed and those over 4BC grade according to Garden and Lane criteria (23) were transferred into the uterine cavity, and then SCM samples (20 μl each) were collected. The procedure was non-invasive. No additional manipulation was performed on the embryos and the development of the embryos was not affected. Furthermore, the embryos were cultured *in vitro* for 5 days, in line with the guidelines of the International Society for Stem Cell Research (https://www.isscr.org/policy/guidelines-for-stem-cell-research-and-clinical-translation). The SCM samples were divided into two groups: Blastocysts that were implanted and those that were not implanted, according to whether a positive fetal heartbeat was observed beyond 8 weeks of gestation. The inclusion criteria were as follows: Age <38 years, and infertility due to tubal obstruction and/or male factors. Patients with recurrent miscarriage; repeated implantation failure; endometriosis; polycystic ovary syndrome; hydrosalpinx; chronic endometritis; immune diseases, such as antiphospholipid syndrome and systemic lupus erythematous; and thrombophilia were excluded. Cycles with two blastocysts transferred at once were included if the blastocysts had the same pregnancy outcomes. The protocol was approved by the Research Ethics Committee of The Fourth Hospital of Shijiazhuang Affiliated to Hebei Medical University (approval no. 20210015). Written informed consent was obtained from all patients before SCM collection. The general characteristics of the patients and blastocysts are presented in Table I.

miRNA isolation and detection from SCM. miRNAs were extracted from the SCM using the miRNeasy Serum/Plasma kit (cat. no. 217184; Qiagen GmbH) according to the manufacturer's instructions. The primers of six miRNAs [miR-372-3p (cat. no. miRA1001610), miR-373-3p (cat. no. miRA1000499), miR-516b-5p (cat. no. miRA1001751), miR-517a-3p (cat. no. miRA100227), miR-519d-3p (cat. no. miRA1001371) and miR-520a-3p (cat. no. miRA100263)] were designed and purchased from Guangzhou RiboBio Co., Ltd. Cel-miR-39-3p (5'-UCACCGGGUGUAAAUCAGCUUG-3'; cat. no. 219600; Qiagen GmbH) was added to each isolation at the time of RNA extraction to serve as an internal control for normalization analysis. The primers for Cel-miR-39-3p were provided by Qiagen GmbH in the miRNeasy Serum/Plasma kit (cat. no. 217184). The detection of miRNAs was performed by reverse transcription-quantitative PCR (RT-qPCR) using miDETECT A Track™ miRNA qRT-PCR Starter kit (cat. no. C10712; Guangzhou RiboBio Co., Ltd.). In total, 162 individual SCM samples were collected, for the first analysis, three SCM pools (n=10 samples each) from the implanted group and three pools from the not-implanted group were created and the six miRNAs were subjected to RT-qPCR. For the second analysis, the remaining 102 individual SCM samples, including 52 from the implanted group and 50 from the not-implanted group were assessed for miR-372-3p, miR-373-3p and miR-519d-3p according to the results of the first analysis. Reactions were performed on a CFX96 Thermal Cycler Dice™ real-time PCR system (Bio-Rad Laboratories, Inc.) under the following parameters: 95˚C for 10 min; followed by 40 cycles at 95˚C for 2 sec, 60˚C for 20 sec and 70˚C for 10 sec. The miRNAs expression was determined using the $2^{-\Delta\Delta Cq}$ method (24) with the implanted group used as the control.

Endometrial sample collection. A total of six women undergoing hysteroscopy for cesarean section scar diverticulum or patients who underwent IVF due to changes in the fallopian tubes were recruited between March and April 2021 at The Fourth Hospital

Table I. Patient characteristics and blastocyst information.

Baseline variables	Implanted group (n=57)	Not-implanted group (n=55)	P-value
Age, years	31.19±4.03	30.87±4.23	0.69
Body mass index, kg/m^2	24.49±3.80	24.04±3.60	0.53
Duration of infertility, years	3.18±2.47	2.96±2.01	0.98
Infertility factors, n (%)			0.86
Female	32 (56.14)	32 (58.18)	
Male	8 (14.04)	9 (16.36)	
Both	17 (29.82)	14 (25.45)	
Fertilization methods, n (%)			0.95
IVF	38 (66.67)	37 (67.27)	
ICSI	19 (33.33)	18 (32.73)	
No. of embryos transferred, n (%)			0.87
One	32 (56.14)	30 (54.55)	
Two	25 (43.86)	25 (45.45)	
Blastocyst grading, n (%)			0.44
≥4BB	57 (69.51)	60 (75.00)	
4BC	25 (30.49)	20 (25.00)	

ICSI, intracytoplasmic sperm injection; IVF, *in vitro* fertilization.

of Shijiazhuang Affiliated to Hebei Medical University. Written informed consent was obtained from all patients before endometrium collection. All the subjects (age range, 18-38 years; mean, 30.5±2.01) with regular menstrual cycles and none of them had received steroid hormone therapy within the previous 3 months. Women with endometrial abnormalities, polycystic ovary syndrome and endometriosis were excluded. The endometrium was obtained from the functional layer of the endometrium during proliferative (n=3) or mid-secretory (n=3) phases of the menstrual cycle. The specimens were immediately fixed in 4% formalin at room temperature for 24 h, then embedded in paraffin. Dating of the menstrual cycle was established by an experienced gynecological pathologist and all of the biopsies showed no evidence of endometrial dysfunction.

Cell culture. The human endometrial cancer cell line (Ishikawa) and placental choriocarcinoma cell line (JAR) were obtained from BeNa Culture Collection (Beijing Beina Chunglian Institute of Biotechnology) and were cultured in DMEM and RPMI-1640 medium (Invitrogen; Thermo Fisher Scientific, Inc.), respectively, supplemented with 10% FBS (cat. no. 11011-8611; Zhejiang Tianhang Biotechnology Co., Ltd.), 100 U/ml penicillin and 100 μg/ml streptomycin (cat. no. P1400; Beijing Solarbio Science & Technology Co., Ltd.) at 37˚C in a humidified incubator under normoxic conditions (95% room air; 5% CO_2). Cells were passaged every 3-4 days at ~80% confluence, and experiments were performed between passage numbers 3 and 5. To mimic hypoxic conditions, Ishikawa cells were maintained in a humidified incubator at 37˚C with 1% O_2, 5% CO_2 and 94% N_2 for 12, 24 or 48 h depends on the needs of the experiments. Both cell lines used in the present study were authenticated by short tandem repeat analysis.

miR-519d-3p uptake by Ishikawa cells. miRNA uptake assay was performed according to previous studies (14,25). Briefly, Cy3-tagged miR-519d-3p and negative control (NC) mimics (the sequences are listed in Table SI) (Shanghai GenePharma Co., Ltd.) were transfected into JAR cells (at 80% confluency) at a concentration of 100 nm using Lipofectamine® 2000 at 37˚C (cat. no. 11668019; Invitrogen; Thermo Fisher Scientific, Inc.). Following 6 h transfection, the cells were washed three times with phosphate-buffered saline (PBS) and incubated with fresh culture media for another 12 h. JAR cells were then harvested and total RNA was extracted for detection of miR-519d-3p by RT-qPCR. Subsequently, Ishikawa cells at 50% confluency were treated with the conditioned media (CM) from JAR cells for 24 h at 37˚C. The assessment of miR-519d-3p uptake by Ishikawa cells was repeated three times and confirmed by RT-qPCR. Visualization of Cy3-miR-519d-3p and NC- mimics uptake was confirmed using immunofluorescence. Briefly, the Ishikawa cells were grown on the coverslips and incubated with CM from JAR cells, as aforementioned. Following treatment, media was removed and cells were washed three times with PBS and fixed with 4% paraformaldehyde for 20 min at room temperature. Nuclei were stained with DAPI (cat. no. G1012; Wuhan Servicebio Technology Co., Ltd.) for 10 min at room temperature, and images were captured using an FV3000 confocal microscope (Olympus Corporation) with a 200x objective lens [numerical aperture(NA) of objective: 0.75].

Transfection. miR-519d-3p mimics, anti-miR-519d-3p, NC of mimics or inhibitor, FUT7-targeted small interfering RNA (siRNA), siRNA NC, HIF1α overexpression plasmid (pcDNA3.1/HIF1α) and the empty vector were purchased from GenePharma co., Ltd. (Suzhou, China). The sequences of

RNA oligonucleotides were listed in Table SI. Ishikawa cells were seeded into 12-well plates ($1.5x10^5$ cells/well); at 80-90% confluence, they were transfected using Lipofectamine® 2000 at 37˚C for 48 and 72 h for RT-qPCR and western blot analysis, respectively, according to the manufacturer's instructions. miR-519d-3p mimics and NC-mimics were used at a concentration of 100 nM, anti-miR-519d-3p and NC-inhibitor at a concentration of 200 nM, FUT7 siRNA and NC-siRNA at a concentration of 50 nm, HIF1α plasmid and the empty vector were used at 1.5 μg/well.

Cell adhesion assay. Ishikawa cells ($1.5x10^5$ cells) were seeded into 12-well plates and cultured for 24 h to form a confluent monolayer (100% confluence). JAR cells ($1x10^5$ cells) were collected and stained with Calcein, AM (cat. no. 40719ES50; Shanghai Yeasen Biotechnology Co., Ltd.) for 30 min at 37˚C. After washing three times with PBS, JAR cells were suspended in 500 μl RMI-1640 medium and delivered gently onto the Ishikawa cell monolayer. After co-incubation at 37˚C for 1 h, the unattached JAR cells were removed by washing with PBS, whereas the attached JAR cells were visualized under a confocal microscope (FV3000; Olympus Corporation) with a 100x objective lens (NA: 0.4). Five areas were randomly captured for each well and the experiments were repeated five times. The number of attached JAR cells was counted using ImageJ v1.8.0 software (National Institutes of Health).

Dual-luciferase gene reporter assay. HIF1α was predicted to be a potential target gene of miR-519d-3p through TargetScan 3.0 (http://www.targetscan.org) and microBase (http://www.mirbase.org). To further confirm the potential binding site of miR-519d-3p and HIF1α mRNA, wild-type (WT) and mutant type (MUT) 3'UTRs of the human HIF1α gene were cloned into a pmirGLO luciferase reporter vector (E1330; Promega Corporation). Ishikawa cells were cultured in a 12-well plate at a density of $1.5x10^5$ cells/well. At 80% confluence, Ishikawa cells were co-transfected with 100 ng of WT-HIF1α (or MUT- HIF1α) and 50 nM of miR-519d-3p mimics (or NC-mimics) using Lipofectamine® 2000 at 37˚C. After transfection for 24 h, firefly and *Renilla* luciferase activities were measured using the Dual-Luciferase Reporter Assay System (cat. no. E1910; Promega Corporation) following the manufacturer's instructions. Firefly luciferase activity was normalized to *Renilla* luciferase activity.

RNA isolation and RT-qPCR. Total RNA was extracted from cells and tissues with TRIzol® reagent (cat. no. 15596026; Invitrogen; Thermo Fisher Scientific, Inc.). For RT, Hifair® II 1st Strand cDNA Synthesis SuperMix for qPCR (cat. no. 11123ES60; Shanghai Yeasen Biotechnology Co., Ltd.) was used following the manufacturer's instructions. qPCR for these genes was performed using Hieff® qPCR SYBRGreen Master Mix (cat. no. 11201ES08; Shanghai Yeasen Biotechnology Co., Ltd.) with ACTB serving as an internal control under the following parameters: 95˚C for 5 min; followed by 40 cycles at 95˚C for 5 min and 60˚C for 30 sec. Primers for HIF1α, integrin subunit αV (ITGAV), integrin subunit β (ITGB)3, ITGB5, E-cadherin, heparin-binding EGF-like growth factor (HBEGF), FUT4, FUT7, ST3Gal3 and ACTB were obtained from Generay Biotech (Shanghai) Co., Ltd. and are listed in Table SII. The detection of miRNA in cells and tissues was the same as that in SCM, using U6 as an internal reference. miDETECT A Track U6 forward primer (cat. no. miRAN0002) and Uni-Reverse Primer (included in miDETECT A Track™ miRNA qPCR kit) were provided by Guangzhou RiboBio Co., Ltd. The relative mRNA levels were determined using the $2^{-\Delta\Delta Cq}$ method.

Western blot analysis. Tissues or cells were lysed in RIPA buffer containing protease inhibitors (cat. no. R0010; Beijing Solarbio Science & Technology Co., Ltd.), and then centrifuged at 4˚C for 15 min at 12,000 x g. Total protein concentration was quantified using NanoDrop 2000 Spectrophotometer (Thermo Fisher Scientific, Inc.), separated by SDS-PAGE on 10% gels and transferred to polyvinylidene difluoride membranes (MilliporeSigma). The membranes were then incubated with 5% fat-free milk at 37˚C for 1 h, and at 4˚C overnight with the following primary antibodies: Anti-HIF1α (cat. no. ab1; mouse; Abcam; 1:500 dilution), anti-FUT7 (cat. no. MAB64091; mouse; R&D Systems, Inc.; 1:1,000 dilution) and anti-β-actin (cat. no. GB12001; mouse; Wuhan Servicebio Technology Co., Ltd.; 1:1,000 dilution). The membranes were washed three times with Tris-buffered saline containing 0.1% Tween-20 for 10 min, and then incubated with horseradish peroxidase (HRP)-conjugated goat anti-mouse IgG (cat. no. 5450-0011; SeraCare Life Sciences, Inc.; 1:5,000 dilution) for 1 h at room temperature. The protein bands were visualized with ECL western blot detecting reagent (cat. no. 36208ES60; Shanghai Yeasen Biotechnology Co., Ltd.) and semi-quantified using ImageJ v1.8.0 software with β-actin as an internal reference to analyze the expression of each protein.

Flow cytometry. Cells were gently trypsinized and a single-cell suspension was collected. After washing twice with PBS, the cells were incubated with PE-conjugated mouse anti-sialyl-Lewis X (sLe^x) antibody (cat. no. 368107; Biolegend, Inc.; 5 μl/test) for 30 min at room temperature in the dark. Unbound antibodies were removed by washing three times with PBS and the cell mixture was adjusted to 500 μl with PBS. Unstained cells were used as controls. Fluorescence was detected by flow cytometry (BD FACSMelody; BD Biosciences) and analyzed with FlowJo v10 software (FlowJo, LLC).

Ultracentrifugation. Three CM samples (1 ml each) from JAR cells and three pooled SCM samples (1 ml each) from expanded blastocysts without signs of degenerating cells (collected between June 2019 and March 2020) were subjected to differential centrifugation according to a previous study (26). Briefly, the samples were centrifuged in sequence at 4˚C at 300 x g for 10 min, 2,000 x g for 10 min and 10,000 x g for 30 min to remove cells, dead cells and cell debris. The supernatant was then transferred to a new tube and centrifuged at 120,000 x g for 90 min at 4˚C. The pellets containing extracellular vesicles (EVs) were suspended in 200 μl PBS. The supernatant was concentrated to 200 μl using Amicon® Ultra-15 Centrifugal Filter Units (3K) (MilliporeSigma). Total RNA from the supernatant and EVs was extracted using the miRNeasy Serum/Plasma Kit (cat. no. 217184; Qiagen GmbH) and miR-519d-3p levels were analyzed by RT-qPCR.

Immunohistochemistry and immunofluorescence assay. The paraffin-embedded endometrial tissues were sliced into 4-μm sections, deparaffinized and rehydrated, followed by antigen retrieval in boiling citrate buffer (pH 6.0) for 20 min. Tissue sections were then incubated with 3% hydrogen peroxide for 10 min at room temperature to block endogenous peroxidase activity and then blocked with 10% goat serum (cat. no. SP-9000; OriGene Technologies, Inc.) for 1 h at room temperature. The tissues were then incubated with the following primary antibodies: Anti-HIF1α (cat. no. orb99244; rabbit; Biorbyt, Ltd.; 1:400), anti-FUT7 (cat. no. 18197-1-AP; rabbit; Proteintech Group, Inc.; 1:400) and anti-sLe^x (cat. no. sc-32243; mouse; Santa Cruz Biotechnology, Inc.; 1:100) at 4˚C overnight. After washing three times with PBS, sections were incubated with biotinylated goat anti-mouse/anti-rabbit IgG antibodies (cat. no. SP-9000; OriGene Technologies, Inc.) for 1 h at room temperature followed by further incubation with HRP-conjugated streptavidin for 15 min at room temperature. Peroxidase activity was visualized by application of diaminobenzidine substrate for 2-3 min at room temperature. Sections were counterstained with hematoxylin for 20 sec at room temperature, dehydrated and sealed before observation under an Olympus IX73 fluorescence microscope (Olympus Corporation).

For immunofluorescence staining, tissues were prepared in the same manner as for immunohistochemistry. After deparaffinization, rehydration and antigen retrieval, the sections were blocked with 3% BSA (cat. no. GC305006; Wuhan Servicebio Technology Co., Ltd.) for 60 min at room temperature. Subsequently, the sections were incubated with primary antibodies against HIF1α (cat. no. orb99244; rabbit; Biorbyt, Ltd.; 1:400), FUT7 (cat. no. 18197-1-AP; rabbit; Proteintech Group, Inc.; 1:400) and sLex (cat. no. sc-32243; mouse; Santa Cruz Biotechnology, Inc.; 1:100) at 4˚C overnight in a humidified chamber. After washing with PBS three times, the tissue sections were incubated for 1 h at room temperature with the following secondary antibodies: Dylight 488-conjugated anti-mouse IgG (cat. no. RS23210; goat; ImmunoWay Biotechnology Company; 1:1,000) and ATTO 594-conjugated anti-rabbit IgG (cat. no. 611-155-122S; goat; Rockland Immunochemicals, Inc.; 1:1,000). Nuclei were stained with DAPI for 10 min at room temperature. Images were captured under a FV3000 confocal laser scanning microscope (Olympus Corporation) with a 200x objective lens (NA: 0.75). To minimize the background signals and biases, the offset value was set at 4 and all images were captured under the same parameters.

Animal studies. A total of 40 Kunming mice (30 female, 10 male; age, 8-10 weeks; weight, 30-35 g) were obtained from the Animal Center of Hebei Medical University (Shijiazhuang, China) and were maintained at a controlled temperature (22-25˚C) and humidity (50%), under a 12-h light/dark cycle, and provided with free access to water and food. Mice were randomly divided into the D1, D4 and D8 group. Both D1 and D4 group included 12 female mice, of which 6 were used for miR-519d-3p and immunofluorescence analysis, and the other 6 for HIF1a and FUT7 protein expression analysis. Six female mice were included in D8 group for embryo counting. The female and male mice were housed at a ratio of 2:1 at 6:00 p.m. every evening, and the vaginal plugs of female mice were checked the next morning at 8:00 a.m. Mice with clearly visible vaginal plugs were defined as gestation D1. On D3 of pregnancy at 9:00 a.m., the mice were anaesthetized intraperitoneally with sodium pentobarbital (50 mg/kg) and a 20 μl solution containing 1.25 nmol miR-519d-3p agomir was slowly infused into the right uterine horn and the same amount of the NC-agomir was infused into the left uterine horn of the same mouse. On D1 and D4 of pregnancy, mice were sacrificed and the endometrium was collected. On D8 of pregnancy, the number of implanted embryos was counted. Mice were anaesthetized using the aforementioned anesthesia protocol and sacrificed by cervical dislocation. Death was confirmed by the following criteria: Respiratory arrest, cardiac arrest, dilation of the pupils and disappearance of nerve reflex. The animal experiments were approved by the Experimental Animal Ethics Committee of Hebei Medical University (approval no. 20210136), and the NIH Guide for the care and Use of Laboratory Animals, 8th edition (27) was followed rigorously.

Statistical analysis. All data were analyzed using SPSS 21.0 software (IBM Corp.). The *in vitro* experiments were independently repeated at least three times and the data are presented as the mean ± standard deviation. The count data were analyzed by χ^2 test, whereas continuous data were analyzed for two groups by paired Student's t-test, unpaired Student's t-test or Mann-Whitney U test. For multi-group comparisons, one-way ANOVA followed by Tukey's post hoc test was used to assess parametric data, and Kruskal-Wallis test followed by Dunn's test was used to assess non-parametric data. The receiver operating characteristic curve was used to determine the value of miRNAs in predicting pregnancy outcomes. $P<0.05$ was considered to indicate a statistically significant difference.

Results

Embryo-released miRNAs are associated with implantation potential. To determine if embryo-released miRNAs were associated with pregnancy outcomes, a total of 162 single SCM samples were collected from infertile patients who underwent routine IVF/ ICSI-ET and divided into implanted and not-implanted groups according to the clinical pregnancy outcomes. Three SCM pools from the implanted group and three pools from the not-implanted group (n=10 samples each) were tested and six miRNAs, miR-372-3p, miR-373-3p, miR-516b-5p, miR-517a-3p, miR-519d-3p and miR-520a-3p, that could be detected in SCM and might be related to embryo quality according to the previous study (15) were selected for RT-qPCR analysis. Unlike cells or tissues, there is no universal reference for miRNA detection in body fluids; therefore, cel-miR-39 was added to each isolation at the time of RNA extraction to serve as an internal spike-in control for normalization analysis according to previous studies (28,29). All six miRNAs were detected in the pooled samples. The expression levels of miR-372-3p, miR-373-3p and miR-519d-3p in the not-implanted group were 3.33, 2.54 and 4.16 times higher compared with those in the implanted group, whereas miR-516b-5p, miR-517a-3p and miR-520a-3p exhibited no

Table II. Analysis of miRNAs in pooled spent embryo culture medium from implanted vs. not-implanted groups.

miRNAs	Cq values of implanted group (n=3)	Cq values of not-implanted group (n=3)	Fold change ($2^{-\Delta\Delta Cq}$)[a]	P-value
hsa-miR-372-3p	34.40±1.97	31.45±0.70	3.33	0.02
hsa-miR-373-3p	35.09±2.53	32.54±1.03	2.54	0.02
hsa-miR-516b-5p	34.26±2.17	33.18±0.24	1.05	0.91
hsa-miR-517a-3p	33.05±0.58	32.29±0.78	0.75	0.17
hsa-miR-519d-3p	33.16±1.74	29.92±1.10	4.16	0.04
hsa-miR-520a-3p	35.51±1.13	34.43±1.19	0.93	0.70

[a]Fold change was calculated with implanted group as the control group. miR/miRNA, microRNA.

significant differences between the two groups. The mean Cq values of the six miRNAs are listed in Table II. Culture media never exposed to embryos were run in parallel and showed no amplification for any of the tested miRNAs.

To further validate the presence and abundance of miR-372-3p, miR-373-3p and miR-519d-3p in SCM, a total of 102 single SCM samples, including 52 from the implanted group and 50 from the not-implanted group, were analyzed. The detection rate in the implanted and not-implanted groups were 82.69 (n=43/52) vs. 78% (n=39/50) for miR-372-3p, 75 (n=39/52) vs. 82%(n=41/50) for miR-373-3p and 84.62 (n=44/52) vs. 90% (n=45/50) for miR-519d-3p. As shown in Fig. 1A, no significant difference was reported in the mean Cq value of cel-miR-39 between the implanted and not-implanted groups, indicating no difference in the efficiency of RNA extraction and amplification. miR-372-3p and miR-519d-3p were much more abundant in the not-implanted group compared with in the implanted group, whereas there was no significant difference in miR-373-3p (Fig. 1B). Subsequently, a receiver operating characteristic curve analysis was conducted. The area under the curve to discriminate embryos that resulted in successful pregnancy from those that resulted in failed pregnancy was 0.78 for miR-519d-3p and 0.71 for miR-372-3p, suggesting a better predictive value of miR-519d-3p for pregnancy outcomes during IVF/ICSI-ET cycles (Fig. 1C).

Embryo-released miR-519d-3p is taken up by endometrial epithelial cells. To determine if endometrial epithelial cells could take up blastocyst-secreted miRNAs, Cy3-miR-519d-3p mimics and NC-mimics were transfected into JAR cells. The JAR cell culture medium was refreshed 6 h after transfection to remove free oligonucleotides and collected 12 h later. Ishikawa cells were then incubated with the collected CM for 24 h. RT-qPCR showed that the expression levels of miR-519d-3p in JAR cells were significantly increased following transfection with miR-519d-3p mimics (Fig. 2A). Compared with treatment with control (NC-mimics) CM, incubation with Cy3-miR-519d-3p CM increased the expression levels of miR-519d-3p in Ishikawa cells by 35.35 times (Fig. 2B). Fluorescent imaging confirmed the presence of Cy3-miR-519d-3p in the cytoplasm of Ishikawa cells (Fig. 2C).

To explore the possible mechanism by which miR-519d-3p was secreted, ultracentrifugation was performed on JAR cell CM and SCM to separate EVs from the supernatant. Notably, miR-519d-3p expression was significantly higher in EVs than that in the supernatants (Fig. 2D). To exclude the possibility that the detected miR-519d-3p was derived from human serum albumin and other components added to the medium, the culture medium without contact with JAR cells or embryos was also assessed using the same method. As expected, the levels of miR-519d-3p in both the supernatant and EVs were either non-detectable or near the detection limit (data not shown), indicating that miR-519d-3p was derived from trophoblasts or blastocysts, and possibly released into the extracellular environment by EVs.

miR-519d-3p suppresses embryo adhesion through HIF1α. The complex implantation process is initiated by the apposition and adhesion of embryos to the uterine endometrial epithelium. Having observed the differential expression of miR-519d-3p in SCM and having determined that miR-519d-3p was taken up by endometrial epithelium cells, it was therefore hypothesized that miR-519d-3p secreted by blastocysts may regulate endometrial gene expression and adhesive properties, which are required for pregnancy success. An established trophoblast-endometrial co-culture adhesion assay was used to investigate the effects of miR-519d-3p on embryo adhesion. Ishikawa cells were transfected with miR-519d-3p mimics, NC-mimics, anti-miR-519d-3p and NC-inhibitor, and untransfected cells were used as a blank control. As embryo implantation and the processes of early pregnancy occur in physiologically hypoxic conditions (30), 48 h after transfection, Ishikawa cells were cultured under hypoxic conditions for another 24 h. As shown in Fig. 3A and B, miR-519d-3p mimics significantly increased the expression levels of miR-519d-3p in Ishikawa cells and inhibited the adhesion of JAR to Ishikawa cells, whereas anti-miR-519d-3p had the opposite effect.

miR-519d-3p has been observed to inhibit embryo adhesion in hypoxia. As the most important transcription factor under hypoxic conditions, HIF1α was reported to be upregulated in endometrium during the implantation window and serves an important role in embryo implantation (31-34). Thus, it was investigated whether HIF1α was a target gene for miR-519d-3p. TargetScan and microBase databases predicted a potential binding site of HIF1α mRNA with miR-519d-3p, which was conserved in different vertebrate species. RT-qPCR and western blot analysis revealed that

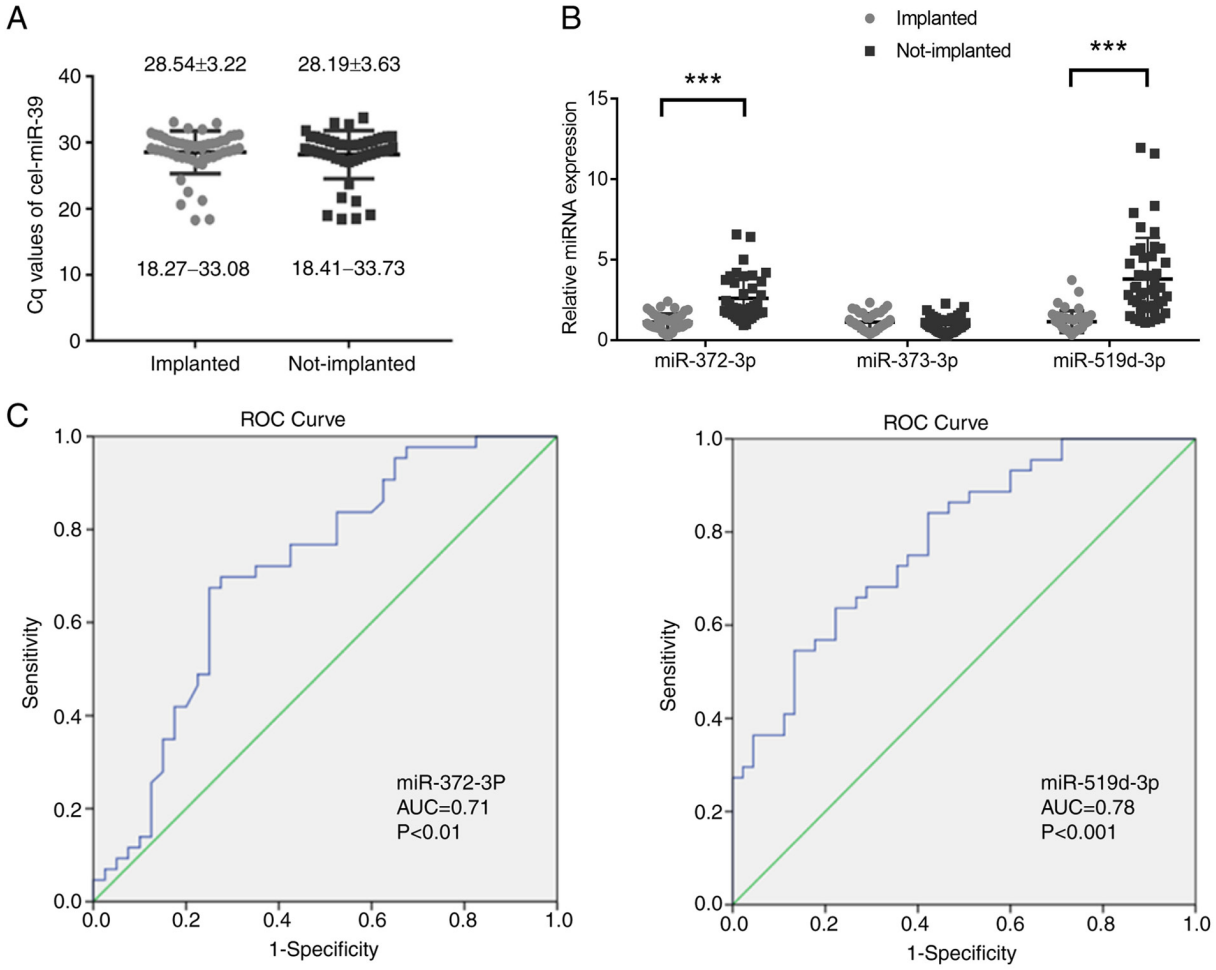

Figure 1. Embryo-released miRNAs are associated with implantation potential. (A) Mean Cq values of cel-miR-39 in implanted and not-implanted groups. (B) $2^{-\Delta\Delta Cq}$ values of miR-372-3p, miR-373-3p and miR-519d-3p in implanted and not-implanted groups. (C) ROC curve analysis of the predictive value of miR-372-3p and miR-519d-3p for embryo implantation. ***P<0.001. AUC, area under the curve; miR, microRNA; ROC, receiver operating characteristic.

miR-519d-3p mimics had no effect on HIF1α mRNA but significantly downregulated HIF1α at the protein level; by contrast, anti-miR-519d-3p upregulated the expression of the HIF1α protein (Fig. 3C and D), indicating that miR-519d-3p did not degrade HIF1α mRNA but inhibited the translation of HIF1α. To verify miR-519d-3p binding directly to the 3'UTR of HIF1α mRNA, the WT or MUT 3'UTR target sequences were cloned into the luciferase reporter vector (pmirGLO) and co-transfected with miR-519d-3p mimics or NC-mimics. As shown in Fig. 3E, luciferase activity was significantly decreased in cells transfected with the HIF1α-WT vector and miR-519d-3p, whereas little change was observed following HIF1α-Mut vector and miR-519d-3p transfection.

To determine whether miR-519d-3p inhibited embryonic adhesion by targeting HIF1α, the pcDNA-HIF1α vector was transfected, or co-transfected with miR-519d-3p mimics, into Ishikawa cells. The protein expression levels of HIF1α were significantly enhanced following pcDNA-HIF1α transfection compared with in cells transfected with the empty vector (Fig. 3F). Upregulation of HIF1α protein increased the number of JAR cells that adhered to Ishikawa cells and partially reversed the inhibitory effect of miR-519d-3p on embryo adhesion (Fig. 3G), suggesting that miR-519d-3p inhibited embryo adhesion by targeting HIF1α under hypoxic conditions.

miR-519d-3p downregulates FUT7 and sLe^x through HIF1α. To further explore the underlying mechanisms of the inhibitory effects of miR-519d-3p on adhesion events, the adhesion-related genes that may be regulated by HIF1α were detected at the transcriptional level. Ishikawa cells were cultured under normoxic or under hypoxic conditions for 12, 24 or 48 h, and the genes associated with embryo adhesion, including ITGAV, ITGB3, ITGB5, E-cadherin, HBEGF (35,36) were detected by RT-qPCR. FUT4, FUT7 (37,38), and ST3Gal3 (39), which participate in the synthesis of oligosaccharide antigen, were also detected. As shown in Fig. 4A, FUT7 mRNA was transcriptionally upregulated under hypoxic conditions in a time-dependent manner. Western blot analysis confirmed that the protein expression levels of FUT7 were increased with the prolongation of hypoxia (Fig. 4B).

FUT7 is a key enzyme for the synthesis of sLe^x, a selectin ligand that has an important role in the initial steps of embryo apposition and adhesion (38). Western blotting and flow cytometry results revealed that miR-519d-3p mimics significantly downregulated the levels of FUT7 and sLe^x (Fig. 4C and D). To clarify the relationship among HIF1α, FUT7 and sLe^x, Ishikawa cells were transfected with FUT7 siRNAs. As shown in Fig. S1, siRNA2 had a significant inhibitory effect on FUT7 protein expression; therefore, this

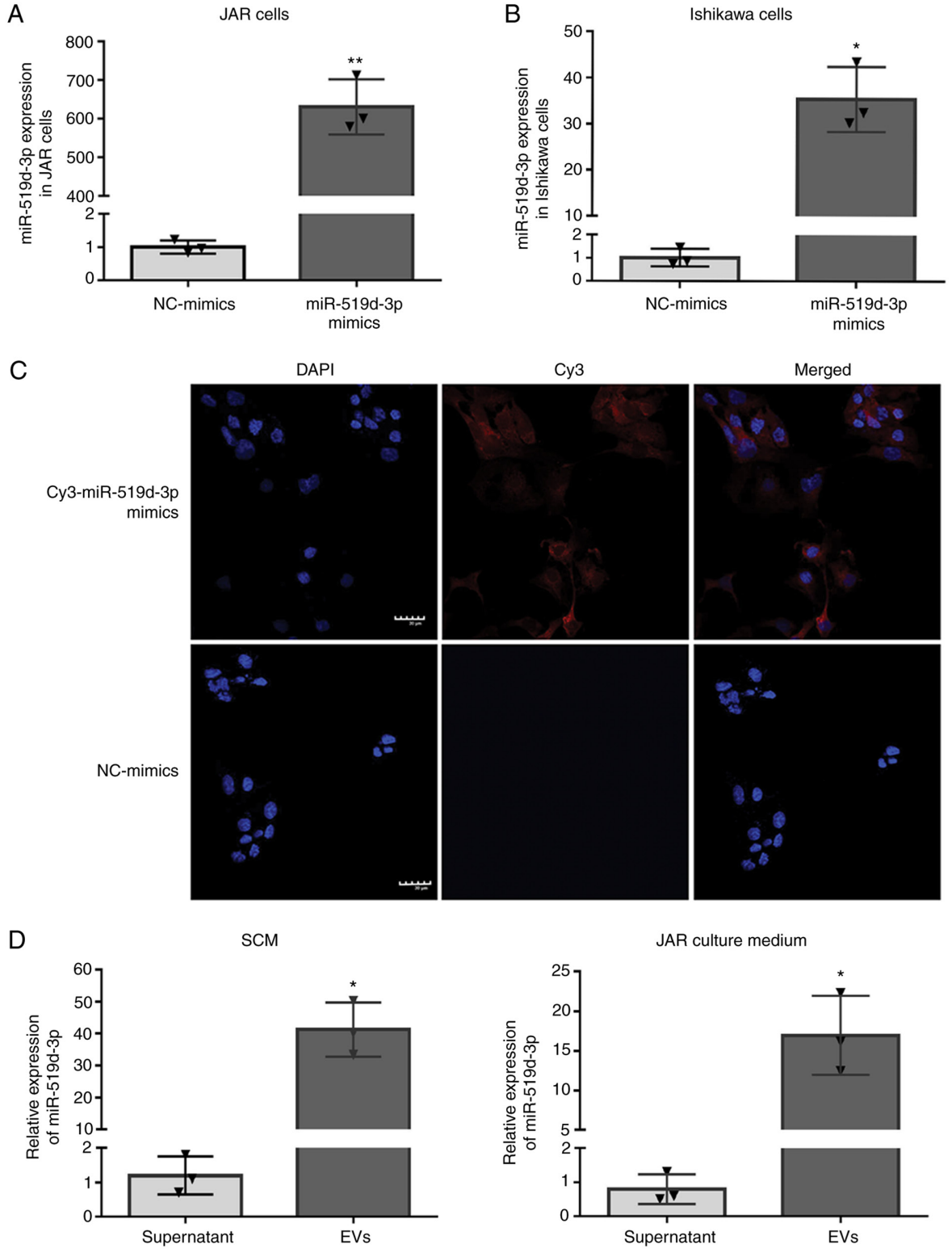

Figure 2. miR-519d-3p released by embryos is taken up by endometrial epithelial cells. (A) Transfection with Cy3-miR-519d-3p mimics increased the levels of miR-519d-3p in JAR cells compared with the NC-mimics. (B) Ishikawa cells, treated with Cy3-miR-519d-3p CM for 24 h, demonstrated a significant increase in miR-519d-3p expression compared with in cells treated with NC-mimics CM. (C) Presence of Cy3-miR-519d-3p in the cytoplasm of Ishikawa cells was visualized using FV3000 confocal microscopy (magnification, x200; NA, 0.75). Scale bars, 30 μm. (D) Expression levels of miR-519d-3p in EVs and the supernatants of SCM and JAR culture medium determined by reverse transcription-quantitative PCR. Each experiment was performed three times. *P<0.05, **P<0.01. CM, conditioned medium; EVs, extracellular vesicles; miR, microRNA; NC, negative control; SCM, spent embryo culture medium.

siRNA was used for subsequent experiments. Compared with in cells transfected with the empty vector, the expression levels of FUT7 protein and sLe^{x} were enhanced by pcDNA-HIF1α transfection, suggesting a positive regulation of FUT7 by HIF1α (Fig. 4E and F). By contrast, co-transfection with pcDNA-HIF1α and FUT7-siRNA decreased the levels of FUT7 and sLe^{x} in Ishikawa cells, and decreased their adhesion to JAR cells in comparison with the pcDNA-HIF1α group

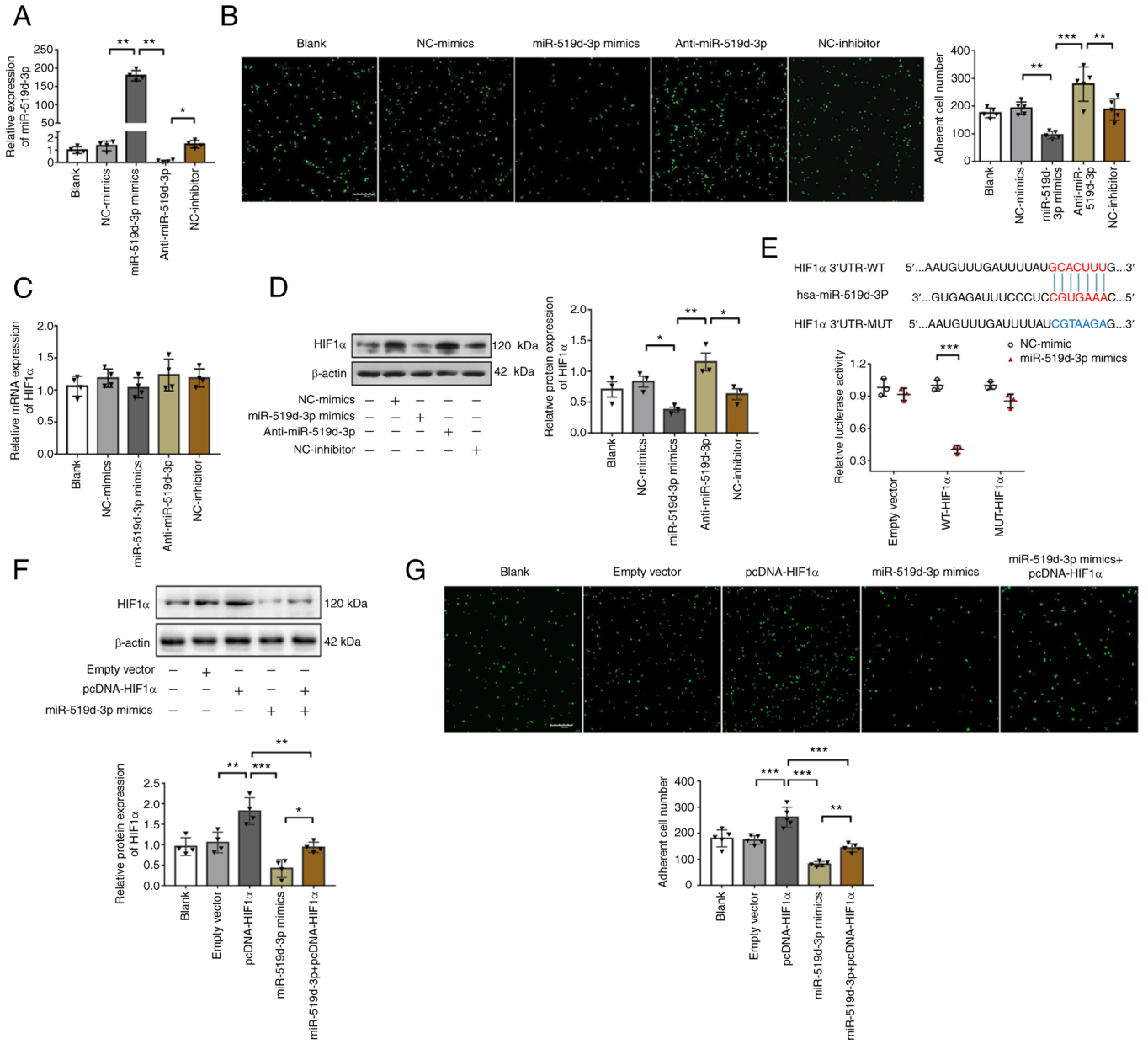

Figure 3. miR-519d-3p suppresses embryo adhesion under hypoxic conditions by targeting HIF1α. (A) Expression levels of miR-519d-3p in Ishikawa cells transfected with miR-519d-3p mimics and anti-miR-519d-3p. (B) Number of adhered JAR cells to Ishikawa cells among the different groups (magnification, x100; NA, 0.4). Scale bars, 200 μm. Effect of miR-519d-3p on HIF1α (C) mRNA and (D) protein expression. (E) Target of miR-519d-3p was verified by a dual-luciferase gene reporter assay. (F) Expression levels of HIF1α protein in Ishikawa cells transfected with miR-519d-3p, pcDNA-HIF1α or co-transfected with miR-519d-3p and pcDNA-HIF1α. (G) Number of adhered JAR cells to Ishikawa cells (magnification, 100x; NA, 0.4). Scale bars, 200 μm. *P<0.05, **P<0.01, ***P<0.001. miR, microRNA; MUT, mutant type; NC, negative control; WT, wild-type.

(Fig. 4G), indicating that HIF1α promoted embryo adhesion to some extent by upregulating FUT7 and sLe^{x}.

Immunohistochemistry was also performed to determine the location and expression of HIF1α, FUT7 and sLe^{x} in human endometrium during the proliferative and mid-secretory phases of the menstrual cycle. HIF1α was observed in both glandular epithelial and stromal cells with stronger staining during the mid-secretory phase than that during the proliferative phase. FUT7 and sLe^{x} were also highly expressed during the mid-secretory phase and mainly localized on the luminal and glandular epithelium (Fig. 4H). The upregulation of HIF1α, FUT7 and sLe^{x} during the implantation window suggested their important role in embryo implantation.

miR-519d-3p hampers embryo implantation in vivo. Having revealed that miR-519d-3p inhibited embryo adhesion *in vitro*, the present study further explored the effect of miR-519d-3p on embryo implantation using a mouse model. On D3 of pregnancy, miR-519d-3p agomir was infused into one side of the uterine cavity; as a control, an equal dose of NC-agomir was infused into the other side of the same mouse. On D1 and D4 of pregnancy, mice were sacrificed and the endometrium was collected for miR-519d-3p/HIF1a and FUT7 expression and immunofluorescence analysis. On D8 of pregnancy, mice were sacrificed and the number of implanted embryos was counted. As shown in Fig. 5A and B, miR-519d-3p agomir infusion markedly increased the levels of miR-519d-3p in the uterine

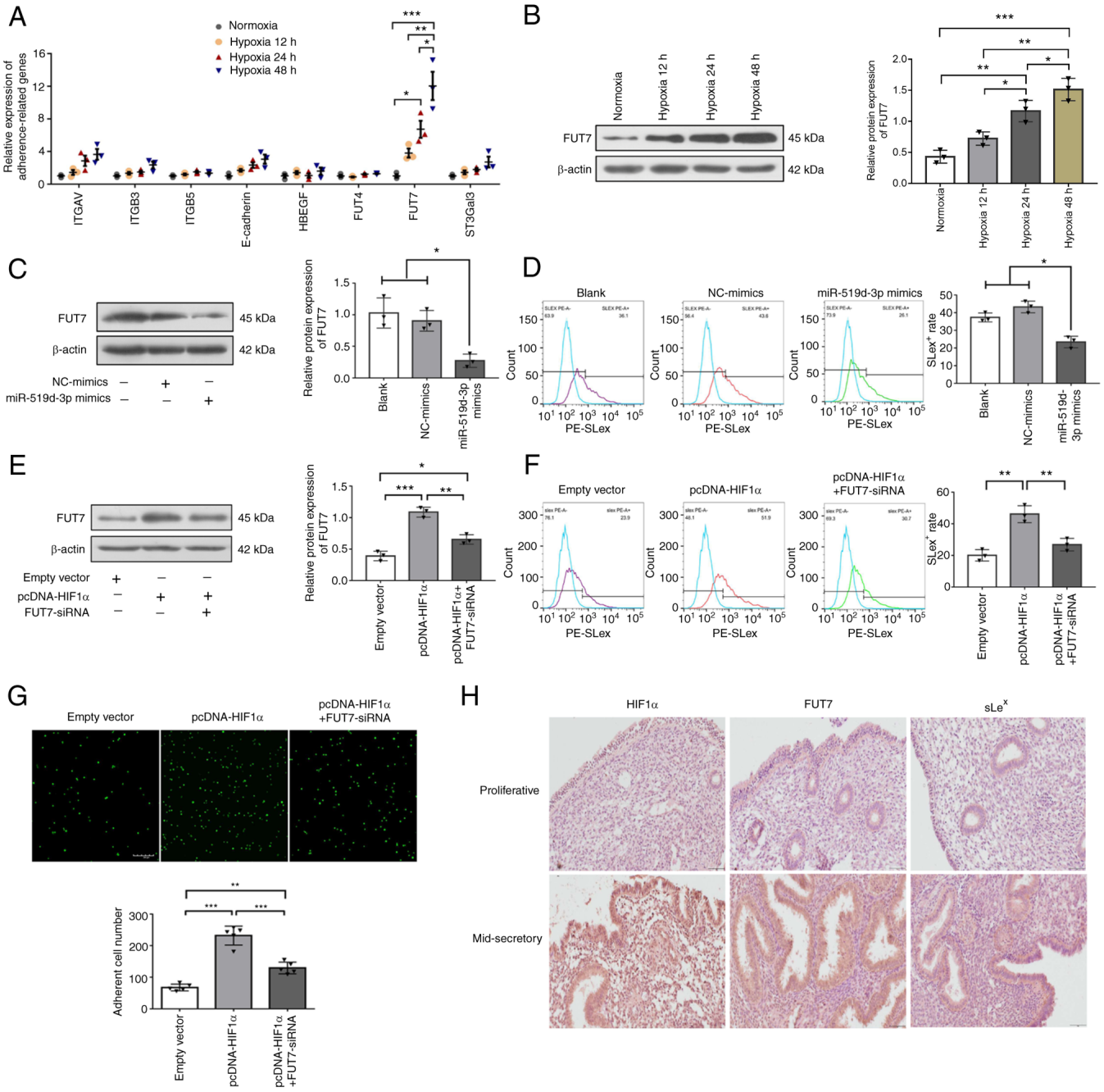

Figure 4. miR-519d-3p downregulates FUT7 and sLe^x by targeting HIF1α, and further inhibits embryo adhesion. (A) Reverse transcription-quantitative PCR analysis of embryo adhesion-related genes under normoxic or hypoxic environments. (B) FUT7 protein expression in Ishikawa cells was increased in a time-dependent manner when exposed to hypoxia. Effect of miR-519d-3p on FUT7 and sLe^x as determined by (C) western blotting and (D) flow cytometry. Levels of (E) FUT7 and (F) sLe^x in Ishikawa cells transfected with the empty plasmid, pcDNA-HIF1α or co-transfected with FUT7-siRNA and pcDNA-HIF1α under normoxic conditions. (G) Number of adhered JAR cells to Ishikawa cells (magnification, x100; NA, 0.4). Scale bars, 200 μm. (H) Immunohistochemical staining (n=3/phase) of HIF1α, FUT7 and sLe^x in human endometrium during the proliferative and mid-secretory phase of the menstrual cycle (magnification, x200). *P<0.05, **P<0.01, ***P<0.001. FUT, fucosyltransferase; HBEGF, heparin-binding EGF-like growth factor; ITGAV, integrin subunit αV; ITGB, integrin subunit β; miR, microRNA; NC, negative control; siRNA, small interfering RNA; sLe^x, sialyl-Lewis X.

endometrium and decreased the number of implanted embryos, compared with in the NC-agomir group. Western blot analysis revealed that HIF1α and FUT7 proteins were at extremely low or undetectable levels in the uterine endometrium on D1 but were significantly enhanced on D4 in the NC-agomir group, which was the window of implantation in the mouse, whereas the enhancement was blocked by miR-519d-3p agomir infusion (Fig. 5C). Immunofluorescence staining displayed similar results. HIF1α, FUT7 and sLe^x were mainly located on the luminal and glandular epithelium with a stronger expression on D4 of pregnancy in the NC-agomir group, but a lower expression detected following miR-519d-3p agomir infusion (Fig. 5D).

Discussion

Effective embryo-endometrium crosstalk is fundamental for successful implantation; however, little is currently known about the precise interaction between the embryo

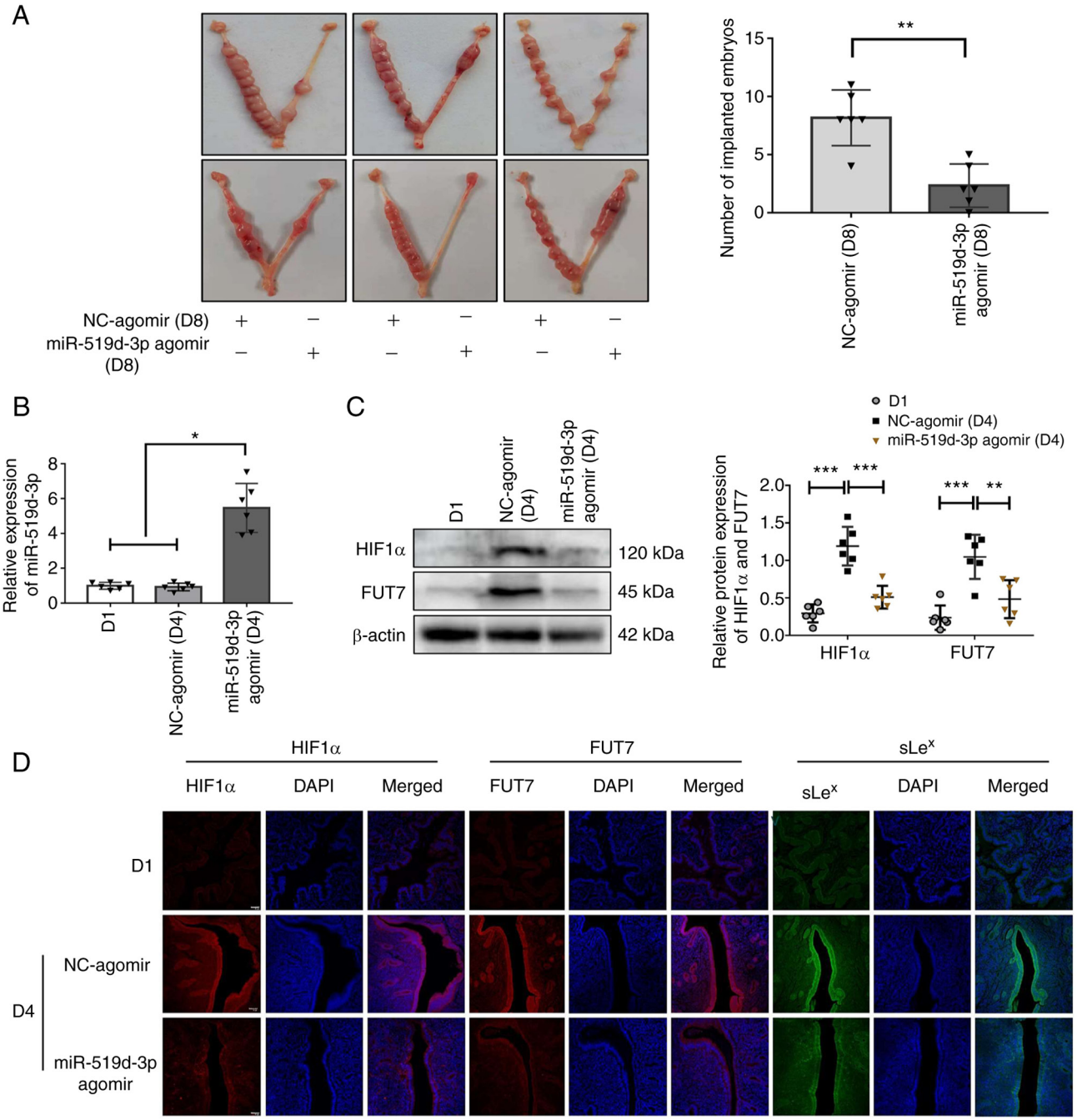

Figure 5. miR-519d-3p inhibits embryo implantation *in vivo*. The right mouse uterine horn was infused with miR-519d-3p agomir, whereas the left side was infused with the NC-agomir. (A) Number of implanted embryos on day 8 of pregnancy. (B) Reverse transcription-quantitative PCR analysis of miR-519d-3p in the uterine endometrium on D1 and D4 of pregnancy. (C) Western blot analysis of HIF1α and FUT7 proteins in mouse endometrium on D1 and D4. (D) Representative images of immunofluorescence staining of HIF1α, FUT7 and sLe^x in mouse endometrium on D1 and D4 (magnification, x200; NA, 0.75). Scale bars, 50 μm. *P<0.05, **P<0.01, ***P<0.001. FUT, fucosyltransferase; miR, microRNA; NC, negative control; sLe^x, sialyl-Lewis X.

and endometrium. The present study, using SCM samples, cell lines and mouse models, demonstrated that miR-372-3p and miR-519d-3p released into the SCM by embryos were negatively associated with implantation potential and may serve as new biomarkers for embryo assessment. Furthermore, miR-519d-3p in the SCM was shown to be taken up by human endometrial epithelial cells and inhibited embryo implantation by targeting HIF1α, which further inhibited the biosynthesis of FUT7 and sLe^x.

How to select embryos with higher implantation potential remains a major challenge in the field of ART. Characterized by high stability and disease-specific expression, the detection of extracellular miRNAs may provide novel and non-invasive biomarkers for embryo quality. Until now, several studies have reported that extracellular miRNAs may be associated with embryo development and implantation (15,16,28,29,40-48). Rosenbluth *et al* (40) detected miRNAs in human SCM for the first time, and revealed that miR-191, miR-645 and miR-372 were much more abundant in SCM from failed embryos compared with those that led to a living birth. Cuman *et al* (14) also identified miR-372 upregulation only in non-implanted SCM samples. By contrast, Fang *et al* (45)

reported that decreased miR-372-3p and miR-373-3p in the SCM was associated with unsuccessful pregnancies. A multicenter study carried out by Cimadomo *et al* (15) tested 10 miRNAs, including the C19MC and miR-371-373 clusters. In contrast to the present results, no clinical predictive power was reported for the miRNAs after adjustment of blastocyst quality and the day of full expansion. Contributing factors to this inconsistency may include the differences in the studied species and populations, differences in fertilization methods, RNA isolation and detection systems. Cimadomo *et al* (15) only analyzed euploid embryos, whereas the present study did not consider the ploidy of embryos. Different miRNA expression profiles between euploid and aneuploid embryos (49) may lead to inconsistent results. Furthermore, to minimize the impact of the endometrium and immune environment on embryo implantation, strict inclusion and exclusion criteria were set in the present study. Patients with tubal obstruction and/or male infertility were included, whereas patients aged ≥38 years, or those with recurrent miscarriage and implantation failures, endometriosis, polycystic ovary syndrome, hydrosalpinx, chronic endometritis, immune diseases such as antiphospholipid syndrome and systemic lupus erythematosus, and thrombophilia were excluded.

Extracellular miRNAs have been reported to bind either to various protein complexes or to be incorporated into EVs, nanoscale membrane vesicles actively released by cells, including exosomes and microvesicles. The special structure of EVs could protect their contents, including proteins, lipids and miRNAs, from degradation in the extracellular environment, thus mediating short-range and long-distance communication between different cells (50). Emerging evidence has demonstrated an important role of EVs in embryo-endometrium communication and embryo implantation (51,52). In the present study, miR-519d-3p was only detectable in the SCM, but not in the culture medium without contact with embryos. Moreover, miR-519d-3p was revealed to be mainly concentrated in the pellets following ultracentrifugation. Using the same method, EVs have been isolated from the SCM in previous studies (26,28), thus suggesting that miR-519d-3p was probably released by embryos encapsulated in EVs. However, another study reported that miR-661 in the SCM was bound to Ago1 protein (14), implying diverse transport mechanisms for different miRNAs, which remains to be further investigated.

miR-519d-3p is a member of the C19MC, which is unique to primates and mainly expressed in embryonic stem cells (53) and later in the placenta (54). The C19MC has been detected in maternal blood as early as 2 weeks after embryo implantation, indicating a critical role in the mother-fetus interface (55). miR-519d-3p has been implicated in the regulation of trophoblast migration and invasion by targeting CXCL6, FOXL2, NR4A2 and MMP2 (56). Its aberrant expression in the placenta or plasma has been reported to be associated with pregnancy pathologies, such as preeclampsia, intrauterine growth restriction and preterm birth (57-60). The present study demonstrated that miR-519d-3p overexpression in endometrial cells hampered embryo adhesion and embryo implantation by targeting HIF1α. HIF1 is an oxygen-regulated transcriptional activator composed of HIF1α and HIF1β subunits. Under hypoxia, HIF1α is activated and various genes associated with adaption to hypoxic stresses, including vascular endothelial growth factor (VEGF), erythropoietin, glucose transporter (GLUT)1 and GLUT3, and insulin-like growth factor 2 can be transcriptionally regulated (61). HIF1α has also been implicated in diverse pathologies, including tumor angiogenesis, migration of cancer cells and brain edema resulting from disruption of water permeability (62). Developing new drugs or miRNAs against this will have huge therapeutic potential for various diseases (63). There is evidence that mice deficient in HIF1 die at the midgestational stage due to vascular defects primarily involving the embryonic and extraembryonic vasculature (64); however, limited studies have focused on the role of HIF1 during early embryo implantation. It has been reported that VEGF, a molecular essential for vascular permeability and angiogenesis, exhibits a similar expression to HIF1 in mouse endometrium during the implantation window (32). Aberrant HIF1α expression and micro-vessel density in human peri-implantation endometrium have been reported to be correlated with repeated miscarriage (33) and recurrent implantation failure (34). Furthermore, altered HIF1α expression and immune localization of GLUT1 and GLUT4 have been found in patients with polycystic ovary syndrome, which may impair glucose uptake and affect decidualization of the endometrium (65). In another study, HIF1α was revealed to induce the expression of prokineticin 1, a crucial regulator of embryo implantation and placentation, via the phosphatidylinositol 3-kinase pathway in endometrial stromal cells (66). All of these findings illustrated the importance of HIF1α during embryo implantation. The present study identified strong expression of HIF1α in the peri-implantation endometrium of both mice and humans. Furthermore, HIF1α overexpression promoted the adhesion of trophoblast cells to endometrial epithelial cells, whereas miR-519d-3p inhibited the process by targeting HIF1α.

During the window of implantation, a variety of molecules are expressed on endometrial epithelial cells to accommodate implanting embryos (35,36). FUTs are a class of enzymes responsible for glycoprotein fucosylation, which have an essential role in determining the stability of the maternal-fetal interface (67). FUT7 has been reported to promote sLe^x-mediated embryo adhesion and embryo implantation (68). sLe^x is a cell-surface oligosaccharide that serves as a common ligand for L-selectin, E-selectin and P-selectin. sLe^x participates in a variety of physiological and pathological processes by interacting with selectins, such as lymphocyte homing, leukocyte exudation in inflammation and metastasis of tumors (69,70). In addition, sLe^x/L-selectin may mediate the initial recognition and adhesion between the embryo and uterus. During the implantation window, sLe^x has been shown to be upregulated in endometrial epithelial cells, especially in the luminal epithelium. In addition, human trophoblast cells incubated from the zona pellucida begin to express L-selectin. The interaction of sLe^x/L-selectin causes the embryonic cells to roll and eventually adhere to the endometrial epithelium (38). Patients with low sLe^x levels in the endometrium tend to have adverse pregnancy outcomes (71,72). In the present study, the enhanced expression of FUT7 and sLe^x during the implantation window was detected in both human and

mouse endometrium. Furthermore, the results suggested that the miR-519d-3p/HIF1a/FUT7/sLe^x signaling pathway endowed embryo selectivity to the endometrium to ensure the implantation of only well-developed embryos.

In conclusion, high levels of miR-372-3p and miR-519d-3p in the SCM were associated with IVF/ICSI failure and may serve as non-invasive biomarkers for embryo selection. Moreover, embryo-released miR-519d-3p provided a new perspective for embryo-mother communication. The role of miR-372-3p was not explored here; sharing the same seed sequence, miR-372-3p may function synergistically with miR-519d-3p. One of the limitations of the present study was the relatively small size of clinical samples and animals assessed. Furthermore, the small amount of SCM sample may be the reason behind the relatively low detection rate. Developing a reliable and sensitive method may help increase the detection rate of miRNAs. Using gene knockout techniques to remove specific miRNA from embryos will help to better clarify the function of miRNA.

Acknowledgements

Not applicable.

Funding

The study was supported by the Key Research and Development Project of Hebei Province (grant no. 213777102D).

Availability of data and materials

The analyzed data sets generated during the study are available from the corresponding author on reasonable request.

Authors' contributions

XHW designed the study and revised the paper. XDW carried out most of the experiments and wrote the paper. SM contributed to the technical support. LL and JY collected spent embryo culture medium and analyzed microRNAs in these samples. SP contributed to the mouse model construction and data analysis. XDW and SP confirmed the authenticity of all the raw data. All authors read and approved the final manuscript.

Ethics approval and consent to participate

The collection of SCM and endometrial tissues was approved by the Research Ethics Committee of the Fourth Hospital of Shijiazhuang Affiliated to Hebei Medical University (Shijiazhuang, China) and written informed consent was obtained from all the participants. The animal experiments were approved by the Experimental Animal Ethics Committee of Hebei Medical University (Shijiazhuang, China).

Patient consent for publication

Not applicable.

Competing interests

The authors declare that they have no competing interests.

References

1. Saha S, Roy P, Corbitt C and Kakar SS: Application of stem cell therapy for infertility. Cells 10: 1613-1638, 2021.
2. Ata B, Kalafat E and Somigliana E: A new definition of recurrent implantation failure on the basis of anticipated blastocyst aneuploidy rates across female age. Fertil Steril 116: 1320-1327, 2021.
3. Carson DD, Bagchi I, Dey SK, Enders AC, Fazleabas AT, Lessey BA and Yoshinaga K: Embryo implantation. Dev Biol 223: 217-237, 2000.
4. Norwitz ER, Schust DJ and Fisher SJ: Implantation and the survival of early pregnancy. N Engl J Med 345: 1400-1408, 2001.
5. Modi DN and Bhartiya P: Physiology of embryo-endometrial cross talk. Biomed Res J 2: 83-104, 2015.
6. Simon C, Gimeno MJ, Mercader A, O'Connor JE, Remohi J, Polan ML and Pellicer A: Embryonic regulation of Integrins b3, a4, and a1 in human endometrial epithelial cells in vitro. J Clin Endocrinol Metab 82: 2607-2616, 1997.
7. Vilella F, Moreno-Moya JM, Balaguer N, Grasso A, Herrero M, Martinez S, Marcilla A and Simon C: Hsa-miR-30d, secreted by the human endometrium, is taken up by the pre-implantation embryo and might modify its transcriptome. Development 142: 3210-3221, 2015.
8. Giglio S, De Nunzio C, Cirombella R, Stoppacciaro A, Faruq O, Volinia S, Baldassarre G, Tubaro A, Ishii H, Croce CM and Vecchione A: A preliminary study of micro-RNAs as minimally invasive biomarkers for the diagnosis of prostate cancer patients. J Exp Clin Cancer Res 40: 79, 2021.
9. Sanchez-Ceinos J, Rangel-Zuniga OA, Clemente-Postigo M, Podadera-Herreros A, Camargo A, Alcala-Diaz JF, Guzman-Ruiz R, Lopez-Miranda J and Malagon MM: miR-223-3p as a potential biomarker and player for adipose tissue dysfunction preceding type 2 diabetes onset. Mol Ther Nucleic Acids 23: 1035-1052, 2021.
10. Yamada NO and Senda T: Circulating microRNA-92a-3p in colorectal cancer: A review. Med Mol Morphol 54: 193-202, 2021.
11. Mori MA, Ludwig RG, Garcia-Martin R, Brandao BB and Kahn CR: Extracellular miRNAs: From biomarkers to mediators of physiology and disease. Cell Metab 30: 656-673, 2019.
12. Zhou W and Dimitriadis E: Secreted MicroRNA to predict embryo implantation outcome: From research to clinical diagnostic application. Front Cell Dev Biol 8: 586510, 2020.
13. Bridi A, Andrade GM, Del Collado M, Sangalli JR, de Avila A, Motta IG, da Silva JCB, Pugliesi G, Silva LA, Meirelles FV, *et al*: Small extracellular vesicles derived from in vivo- or in vitro-produced bovine blastocysts have different miRNAs profiles-Implications for embryo-maternal recognition. Mol Reprod Dev 88: 628-643, 2021.
14. Cuman C, Van Sinderen M, Gantier MP, Rainczuk K, Sorby K, Rombauts L, Osianlis T and Dimitriadis E: Human blastocyst secreted microRNA regulate endometrial epithelial cell adhesion. EBioMedicine 2: 1528-1535, 2015.
15. Cimadomo D, Rienzi L, Giancani A, Alviggi E, Dusi L, Canipari R, Noli L, Ilic D, Khalaf Y, Ubaldi FM and Capalbo A: Definition and validation of a custom protocol to detect miRNAs in the spent media after blastocyst culture: Searching for biomarkers of implantation. Hum Reprod 34: 1746-1761, 2019.
16. Capalbo A, Ubaldi FM, Cimadomo D, Noli L, Khalaf Y, Farcomeni A, Ilic D and Rienzi L: MicroRNAs in spent blastocyst culture medium are derived from trophectoderm cells and can be explored for human embryo reproductive competence assessment. Fertil Steril 105: 225-235 e1-3, 2016.
17. Paquette AG, Chu T, Wu X, Wang K, Price ND and Sadovsky Y: Distinct communication patterns of trophoblastic miRNA among the maternal-placental-fetal compartments. Placenta 72-73: 28-35, 2018.
18. Delorme-Axford E, Donker RB, Mouillet JF, Chu T, Bayer A, Ouyang Y, Wang T, Stolz DB, Sarkar SN, Morelli AE, *et al*: Human placental trophoblasts confer viral resistance to recipient cells. Proc Natl Acad Sci USA 110: 12045-12053, 2013.
19. Jing J, Wang Y, Quan Y, Wang Z, Liu Y and Ding Z: Maternal obesity alters C19MC microRNAs expression profile in fetal umbilical cord blood. Nutr Metab (Lund) 17: 52, 2020.
20. Kambe S, Yoshitake H, Yuge K, Ishida Y, Ali MM, Takizawa T, Kuwata T, Ohkuchi A, Matsubara S, Suzuki M, *et al*: Human exosomal placenta-associated miR-517a-3p modulates the expression of PRKG1 mRNA in Jurkat cells1. Biol Reprod 91: 129, 2014.

21. Chaiwangyen W, Murrieta-Coxca JM, Favaro RR, Photini SM, Gutiérrez-Samudio RN, Schleussner E, Markert UR and Morales-Prieto DM: MiR-519d-3p in trophoblastic cells: Effects, targets and transfer to allogeneic immune cells via extracellular vesicles. Int J Mol Sci 21: 3458, 2020.
22. Morales-Prieto DM, Ospina-Prieto S, Chaiwangyen W, Schoenleben M and Markert UR: Pregnancy-associated miRNA-clusters. J Reprod Immunol 97: 51-61, 2013.
23. Gardner DK and Lane M: Culture and selection of viable blastocysts: A feasible proposition for human IVF? Hum Reprod Update 3: 367-382, 1997.
24. Livak KJ and Schmittgen TD: Analysis of relative gene expression data using real-time quantitative PCR and the 2(-Delta Delta C(T)) method. Methods 25: 402-408, 2001.
25. Zhou J, Li YS, Nguyen P, Wang KC, Weiss A, Kuo YC, Chiu JJ, Shyy JY and Chien S: Regulation of vascular smooth muscle cell turnover by endothelial cell-secreted microRNA-126: Role of shear stress. Circ Res 113: 40-51, 2013.
26. Giacomini E, Vago R, Sanchez AM, Podini P, Zarovni N, Murdica V, Rizzo R, Bortolotti D, Candiani M and Viganò P: Secretome of in vitro cultured human embryos contains extracellular vesicles that are uptaken by the maternal side. Sci Rep 7: 5210, 2017.
27. National Research Council (US) Committee for the Update of the Guide for the Care and Use of Laboratory Animals: Guide for the Care and Use of Laboratory Animals. Vol 8. National Academies Press (US), Washington, DC, 2011. https://grants.nih.gov/grants/olaw/Guide-for-the-Care-and-use-of-laboratory-animals.pdf
28. Abu-Halima M, Häusler S, Backes C, Fehlmann T, Staib C, Nestel S, Nazarenko I, Meese E and Keller A: Micro-ribonucleic acids and extracellular vesicles repertoire in the spent culture media is altered in women undergoing in vitro fertilization. Sci Rep 7: 13525, 2017.
29. Gross N, Kropp J and Khatib H: Sexual dimorphism of miRNAs secreted by bovine in vitro-produced embryos. Front Genet 8: 39, 2017.
30. Fischer B and Bavister BD: Oxygen tension in the oviduct and uterus of rhesus monkeys, hamsters and rabbits. J Reprod Fertil 99: 673-679, 1993.
31. Salman MM, Kitchen P, Woodroofe MN, Bill RM, Conner AC, Heath PR and Conner MT: Transcriptome analysis of gene expression provides new insights into the effect of mild therapeutic hypothermia on primary human cortical astrocytes cultured under hypoxia. Front Cell Neurosci 11: 386-400, 2017.
32. Daikoku T, Matsumoto H, Gupta RA, Das SK, Gassmann M, DuBois RN and Dey SK: Expression of hypoxia-inducible factors in the peri-implantation mouse uterus is regulated in a cell-specific and ovarian steroid hormone-dependent manner. Evidence for differential function of HIFs during early pregnancy. J Biol Chem 278: 7683-7691, 2003.
33. Chen X, Jiang L, Wang CC, Huang J and Li TC: Hypoxia inducible factor and microvessels in peri-implantation endometrium of women with recurrent miscarriage. Fertil Steril 105: 1496-1502. e4, 2016.
34. Yu X, Gao C, Dai C, Yang F and Deng X: Endometrial injury increases expression of hypoxia-inducible factor and angiogenesis in the endometrium of women with recurrent implantation failure. Reprod Biomed Online 38: 761-767, 2019.
35. Rarani FZ, Borhani F and Rashidi B: Endometrial pinopode biomarkers: Molecules and microRNAs. J Cell Physiol 233: 9145-9158, 2018.
36. Koot YE, Teklenburg G, Salker MS, Brosens JJ and Macklon NS: Molecular aspects of implantation failure. Biochim Biophys Acta 1822: 1943-1950, 2012.
37. Zheng Q, Zhang D, Yang YU, Cui X, Sun J, Liang C, Qin H, Yang X, Liu S and Yan Q: MicroRNA-200c impairs uterine receptivity formation by targeting FUT4 and alpha1,3-fucosylation. Cell Death Differ 24: 2161-2172, 2017.
38. Genbacev OD, Prakobphol A, Foulk RA, Krtolica AR, Ilic D, Singer MS, Yang ZQ, Kiessling LL, Rosen SD and Fisher SJ: Trophoblast L-selectin-mediated adhesion at the maternal-fetal interface. Science 299: 405-408, 2003.
39. Yu M, Wang H, Liu J, Qin H, Liu S and Yan Q: The sialyltransferase ST3Gal3 facilitates the receptivity of the uterine endometrium in vitro and in vivo. FEBS Lett 592: 3696-3707, 2018.
40. Rosenbluth EM, Shelton DN, Wells LM, Sparks AE and Van Voorhis BJ: Human embryos secrete microRNAs into culture media-a potential biomarker for implantation. Fertil Steril 101: 1493-1500, 2014.
41. Borges E Jr, Setti AS, Braga DP, Geraldo MV, Figueira RC and Iaconelli A Jr: miR-142-3p as a biomarker of blastocyst implantation failure-A pilot study. JBRA Assist Reprod 20: 200-205, 2016.
42. Sanchez-Ribas I, Diaz-Gimeno P, Quinonero A, Ojeda M, Larreategui Z, Ballesteros A and Dominguez F: NGS analysis of human embryo culture media reveals miRNAs of extra embryonic origin. Reprod Sci 26: 214-222, 2019.
43. Heidari F, Hosseini S, Yeganeh SM and Salehi M: Expression of miR-Let-7a, miR-15a, miR-16-1, and their target genes in fresh and vitrified embryos and its surrounding culture media for noninvasive embryo assessment. J Cell Biochem 120: 19691-19698, 2019.
44. Russell SJ, Menezes K, Balakier H and Librach C: Comprehensive profiling of Small RNAs in human embryo-conditioned culture media by improved sequencing and quantitative PCR methods. Syst Biol Reprode Med 66: 129-139, 2020.
45. Fang F, Li Z, Yu J, Long Y, Zhao Q, Ding X, Wu L, Shao S, Zhang L and Xiang W: MicroRNAs secreted by human embryos could be potential biomarkers for clinical outcomes of assisted reproductive technology. J Adv Res 31: 25-34, 2021.
46. Rio PD and Madan P: Does miRNA Expression in the spent media change during early embryo development? Front Vet Sci 8: 658968, 2021.
47. Khan HL, Bhatti S, Abbas S, Kaloglu C, Isa AM, Younas H, Ziders R, Khan YL, Hassan Z, Turhan BO, *et al*: Extracellular microRNAs: Key players to explore the outcomes of in vitro fertilization. Reprod Biol Endocrinol 19: 72, 2021.
48. Hawke DC, Ahmed DB, Watson AJ and Betts DH: Murine blastocysts release mature microRNAs into culture media that reflect developmental status. Front Genet 12: 655882, 2021.
49. Rosenbluth EM, Shelton DN, Sparks AET, Devor E, Christenson L and Van Voorhis BJ: MicroRNA expression in the human blastocyst. Fertil Steril 99: 855-861.e3, 2013.
50. Tkach M and Théry C: Communication by extracellular vesicles: Where we are and where we need to go. Cell 164: 1226-1232, 2016.
51. Kurian NK and Modi D: Extracellular vesicle mediated embryo-endometrial cross talk during implantation and in pregnancy. J Assist Reprod Genet 36: 189-198, 2019.
52. Giacomini E, Makieva S, Murdica V, Vago R and Vigano P: Extracellular vesicles as a potential diagnostic tool in assisted reproduction. Curr Opin Obstet Gynecol 32: 179-184, 2020.
53. Lin S, Cheung WK, Chen S, Lu G, Wang Z, Xie D, Li K, Lin MC and Kung HF: Computational identification and characterization of primate-specific microRNAs in human genome. Comput Biol Chem 34: 232-241, 2010.
54. Liang Y, Ridzon D, Wong L and Chen C: Characterization of microRNA expression profiles in normal human tissues. BMC Genomics 8: 166, 2007.
55. Dumont TMF, Mouillet JF, Bayer A, Gardner CL, Klimstra WB, Wolf DG, Yagel S, Balmir F, Binstock A, Sanfilippo JS, *et al*: The expression level of C19MC miRNAs in early pregnancy and in response to viral infection. Placenta 53: 23-29, 2017.
56. Xie L, Mouillet JF, Chu T, Parks WT, Sadovsky E, Knofler M and Sadovsky Y: C19MC microRNAs regulate the migration of human trophoblasts. Endocrinology 155: 4975-4985, 2014.
57. Hromadnikova I, Kotlabova K, Ivankova K and Krofta L: Expression profile of C19MC microRNAs in placental tissue of patients with preterm prelabor rupture of membranes and spontaneous preterm birth. Mol Med Rep 16: 3849-3862, 2017.
58. Hromadnikova I, Kotlabova K, Ivankova K and Krofta L: First trimester screening of circulating C19MC microRNAs and the evaluation of their potential to predict the onset of preeclampsia and IUGR. PLoS One 12: e0171756, 2017.
59. Hromadnikova I, Dvorakova L, Kotlabova K and Krofta L: The prediction of gestational hypertension, preeclampsia and fetal growth restriction via the first trimester screening of plasma exosomal C19MC microRNAs. Int J Mol Sci 20: 2972, 2019.
60. Wommack JC, Trzeciakowski JP, Miranda RC, Stowe RP and Ruiz RJ: Micro RNA clusters in maternal plasma are associated with preterm birth and infant outcomes. PLoS One 13: e0199029, 2018.
61. Semenza GL: Regulation of mammalian O2 homeostasis by hypoxia-inducible factor 1. Annu Rev Cell Dev Biol 15: 551-578, 1999.
62. Salman MM, Kitchen P, Halsey A, Wang MX, Törnroth-Horsefield S, Conner AC, Badaut J, Iliff JJ and Bill RM: Emerging roles for dynamic aquaporin-4 subcellular relocalization in CNS water homeostasis. Brain 145: 64-75, 2022.

63. Salman MM, Kitchen P, Yool AJ and Bill RM: Recent breakthroughs and future directions in drugging aquaporins. Trends Pharmacol Sci 43: 30-42, 2022.
64. Semenza GL: HIF-1: Mediator of physiological and pathophysiological responses to hypoxia. J Appl Physiol (1985) 88: 1474-1480, 2000.
65. Zhao DM: Analysis of pregnancy outcomes in obese-women with PCOS after IVF-ET and effects of hypoxia-inducible factor-1a on endometrial receptivity of them (unpublished PhD thesis). Shandong University School of Medicine, 2018.
66. Ujvari D, Jakson I, Oldmark C, Attarha S, Alkasalias T, Salamon D, Gidlöf S and Hirschberg AL: Prokineticin 1 is up-regulated by insulin in decidualizing human preendometrial stromal cells. J Cell Mol Med 22: 163-172, 2018.
67. Aplin JD and Jones CJ: Fucose, placental evolution and the glycocode. Glycobiology 22: 470-478, 2012.
68. Zhang Y, Liu S, Liu Y, Wang Z, Wang X and Yan Q: Overexpression of fucosyltransferase VII (FUT7) promotes embryo adhesion and implantation. Fertil Steril 91: 908-914, 2009.
69. Jin F and Wang F: The physiological and pathological roles and applications of sialyl Lewis x, a common carbohydrate ligand of the three selectins. Glycoconj J 37: 277-291, 2020.
70. Li DS, Sun HZ, Bai G, Wang W, Liu MM, Bao ZY, Li JJ and Liu H: α-1,3-Fucosyltransferase-VII siRNA inhibits the expression of SLex and hepatocarcinoma cell proliferation. Int J Mol Med 42: 2700-2708, 2018.
71. Wang B, Sheng JZ, He RH, Qian YL, Jin F and Huang HF: ORIGINAL ARTICLE: High expression of l-selectin ligand in secretory endometrium is associated with better endometrial receptivity and facilitates embryo implantation in human being. Am J Reprod Immunol 60: 127-134, 2008.
72. Foulk RA, Zdravkovic T, Genbacev O and Prakobphol A: Expression of L-selectin ligand MECA-79 as a predictive marker of human uterine receptivity. J Assist Reprod Genet 24: 316-321, 2007.